

Study of dolines of the Cajla Karst originated on covered karst landform (Malé Karpaty Mts., Western Carpathians)

Alexander Lačný^{1,2}, René Putiška³, Rastislav Vojtko², Laura Dušeková^{4,5}, Andrej Mojzeš³, Bibiana Brixová³, Ivan Zvara³, Erik Andrassy³ & Peter Magdolen⁶

¹ State Nature Conservancy of the Slovak Republic, Little Carpathians Protected Landscape Area, Štúrova 115, 900 01 Modra, Slovakia; alexander.lacny@soprs.sk

² Department of Geology and Palaeontology, Faculty of Natural Sciences, Comenius University in Bratislava, Ilkovičova 6, 842 15 Bratislava, Slovakia; alexander.lacny@uniba.sk; rastislav.vojtko@uniba.sk

³ Department of Engineering Geology, Hydrogeology and Applied Geophysics, Faculty of Natural Sciences, Comenius University in Bratislava, Ilkovičova 6, 842 15 Bratislava, Slovakia

⁴ State Nature Conservancy of the Slovak Republic, Slovak Caves Administration, Hodžova 11, 031 01 Liptovský Mikuláš, Slovakia

⁵ Institute of Geodesy, Cartography and Geographical Information Systems, Faculty of Mining, Ecology, Process Control and Geotechnologies, Technical University Košice, Park Komenského 19, 04001 Košice, Slovakia; laura.dusekova@student.tuke.sk

⁶ Cave Group Speleo Bratislava, Košariská 4100, 900 55 Lozorno, Slovakia

AGEOS

Abstract: Presented research investigate the phenomenon of karstic area remarkable with specific karst landform, so-called covered karst. So far, not much attention has been paid to this particular type of karst in Slovakia, so the aim of the research is to bring new information on it, especially on dolines formation and their origin. Study was focused on 50 dolines following the distinctive NE–SW line in the study area - the Cajla Karst located in the Malé Karpaty Mts., Slovakia. To understand the process of the formation of dolines in the covered karst and to distinguish the dolines from the pits resulted from anthropogenic processing via mining, several geophysical methods were adopted to prove the doline origin (soil radon emanometry, electric resistivity tomography and seismic refraction tomography). For identification of dolines and subsequent processing, the lidar data were used. The formation of studied dolines was controlled by lithological-tectonic properties of the bedrock, especially along the contact zone of karstic (Triassic carbonates) and non-karstic rocks composed of quartzite and crystalline basement, predominantly granitic composition. The resulting shape was also influenced by infiltration of surface water into the underground.

Key words: Cajla Karst, dolines, covered karst, lidar data, electric resistivity tomography, seismic refraction tomography, soil radon emanometry

1. INTRODUCTION

Dolines, which are the most distinctive surface forms of the karstic relief, represent closed depressions of variable dimensions with slightly angled or even vertical side walls (Bondesan et al., 1992; Williams, 2004; Waltham et al., 2005; Sauro, 2012). Morphodynamically, dolines represent a basic hydrographic unit, which as a simple catchment area with its system of slopes, drains the water to the lowermost accumulation point (Bondesan et al., 1992; Williams, 2004). The genesis of dolines is influenced by topographic, tectonic, lithological and morphostructural predisposition.

Several methodological approaches have been developed, both for characterisation of ideal parameters for geometric shape and for characterisation of dolines as an integral part of a complex geosystem in relation to geological, geomorphological, hydrological, climatic, pedologic, and biogeographic properties of the land (e.g., Cvijić, 1893; Segre, 1948; Williams, 1972; Castiglioni, 1991; Bondesan et al., 1992).

Therefore, they can originate through several processes. Four major mechanisms of forming dolines are distinguished: corrosion, collapses, suffosion, and subsidence. However, it is not possible to link the origin of dolines with only one process. Therefore, dolines are considered predominantly to be polygenetic relief forms. Depending on the process, a variety of doline

shapes can be documented and they occur either isolated or in groups. Because the international terminology includes more deep-routed terms for genetic types of dolines, Williams (2004) linked the respective terms with specific genetic processes and thus made the nomenclature more transparent.

Based on their shape, dolines were classified according to the work of Jakál (1975). With regards to the inclination of their walls, dolines can be divided into four categories: funnel-shaped, cup-shaped, kettle-shaped, and ring-shaped. Jakál & Bella (2008) distinguish three types of dolines based on their genesis: solution dolines, collapse dolines, alluvial dolines.

The Malé Karpaty Mts. comprise several individual karstic areas (Devín Karst, Borinka Karst, Cajla Karst, Kuchyňa-Orešany Karst, Plavecký Karst, Smolenice Karst, Dobrá Voda Karst, Čachtice Karst) with approximately 500 documented dolines (Mitter, 1983; Hochmuth, 2008). These unique landforms are very characteristic for all karstic regions except the Devín Karst located in the southwestern tip of the mountains. Our research was focused on the Cajla Karst, a small karstic area, which is a part of the Pezinské Karpaty Mts (Fig. 1). Previously, only a little attention was paid to this area, possibly because of a rather limited extent of identified underground karstic forms. Part of this karstic area, where dolines are located is remarkable with specific karst landform, so-called covered karst.

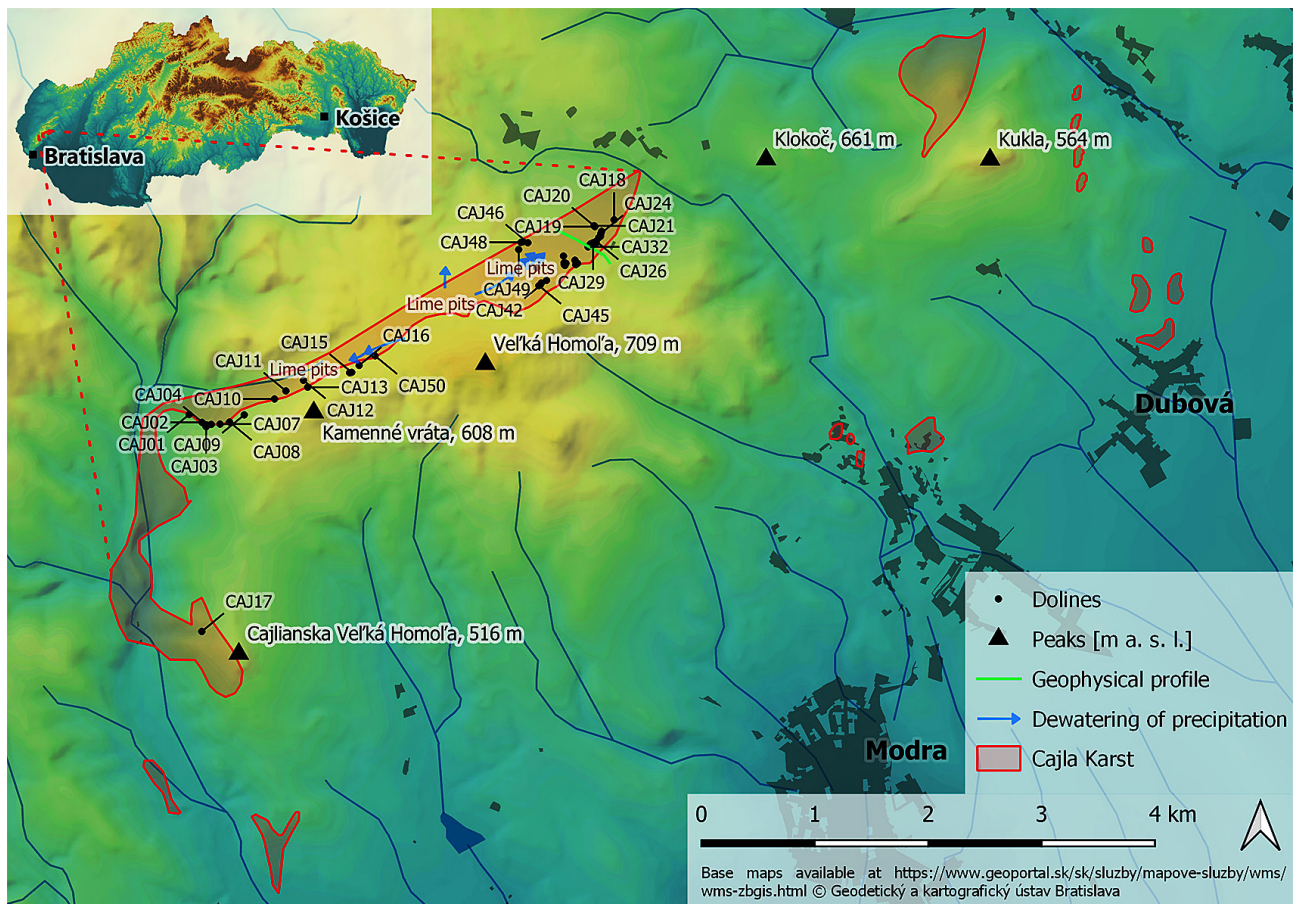


Fig. 1. Schematic figure of the Cajla Karst with the mapped dolines in the central part of the Malé Karpaty Mts. and insert map with location of the study area within Slovakia.

Many authors have classified covered karst (e.g., Gvozdetzkiy, 1965; Quinlan, 1978; Hevesi, 1986; White, 1988; Veress, 2016, 2020). According to Hevesi (1986), if there is non-karstic cover on the karst, it may be covered, non-individual (there is no karstic rock at the surface) and partly covered. He distinguished buried karst or closed karst (the cover is impermeable) and concealed karst (the cover is permeable) within covered, non-individual karst. Veress (2016) distinguished four varieties of cryptokarst: allogenic cryptokarst, autogenic cryptokarst, transitional cryptokarst and cryptokarst developed from buried karst.

Covered karsts are classified according to the character of the cover (cryptokarst = the cover is impermeable; concealed karst = the cover is permeable); the origin of cover deposits (locally deposited or transported there); and the age of karstification (syngenetic = the depression in the cover and the form in the bedrock are of the same age; postgenetic = they are not of the same age) (Veress, 2016). The covered karst can be covered by sediments not derived from karst, either unconsolidated or consolidated, but developed independently from the limestone, i.e., the bedrock underlying the karst. In Slovakia, similarly focused research of the covered karst has not been performed to date. However, several studies from abroad have been performed lately, focusing on the study of specific regions with the covered karst and dolines present on its surface (e.g., Kruse et al., 2006; Upchurch et al., 2013; Trájer, 2020).

In the Cajla Karst, there are several tens of dolines, which were the focus of our research. Some of these dolines are rather specific in form. In general, dolines have been rarely studied in Slovakia. Several geophysical methods were tested to elucidate the formation of dolines.

2. GEOLOGY AND GEOMORPHOLOGY

The Malé Karpaty Mts. form the southwestern end of the Carpathian arc in Europe. The mountains are traditionally divided, from the south to the north, into the Devínske Karpaty Mts., Pezinské Karpaty Mts., Brezovské Karpaty Mts., and Čachtické Karpaty Mts. and belong to the Fatra-Tatra geomorphological area (Mazúr & Lukniš, 1978). Geomorphologically, the Cajla Karst belongs to Malé Karpaty Mts. subunit Pezinské Karpaty, and part of Homolské Karpaty Mts., respectively (Mazúr & Lukniš, 1978). According to our research, most of the studied dolines are located in the area which reaches mean value of slope from 6 to 10 degrees. The area of the whole Cajla Karst, based on geological map at a scale of 1:50,000 (2013), is ca 3.02 km².

The study area (Figs. 2, 3, 4) is built up by the Eo-Alpine Tatric Unit, which is composed of the Variscan crystalline basement and the cover sequence (Plašienka et al., 1991). The crystalline basement contains Lower Palaeozoic metabasites, metamorphosed

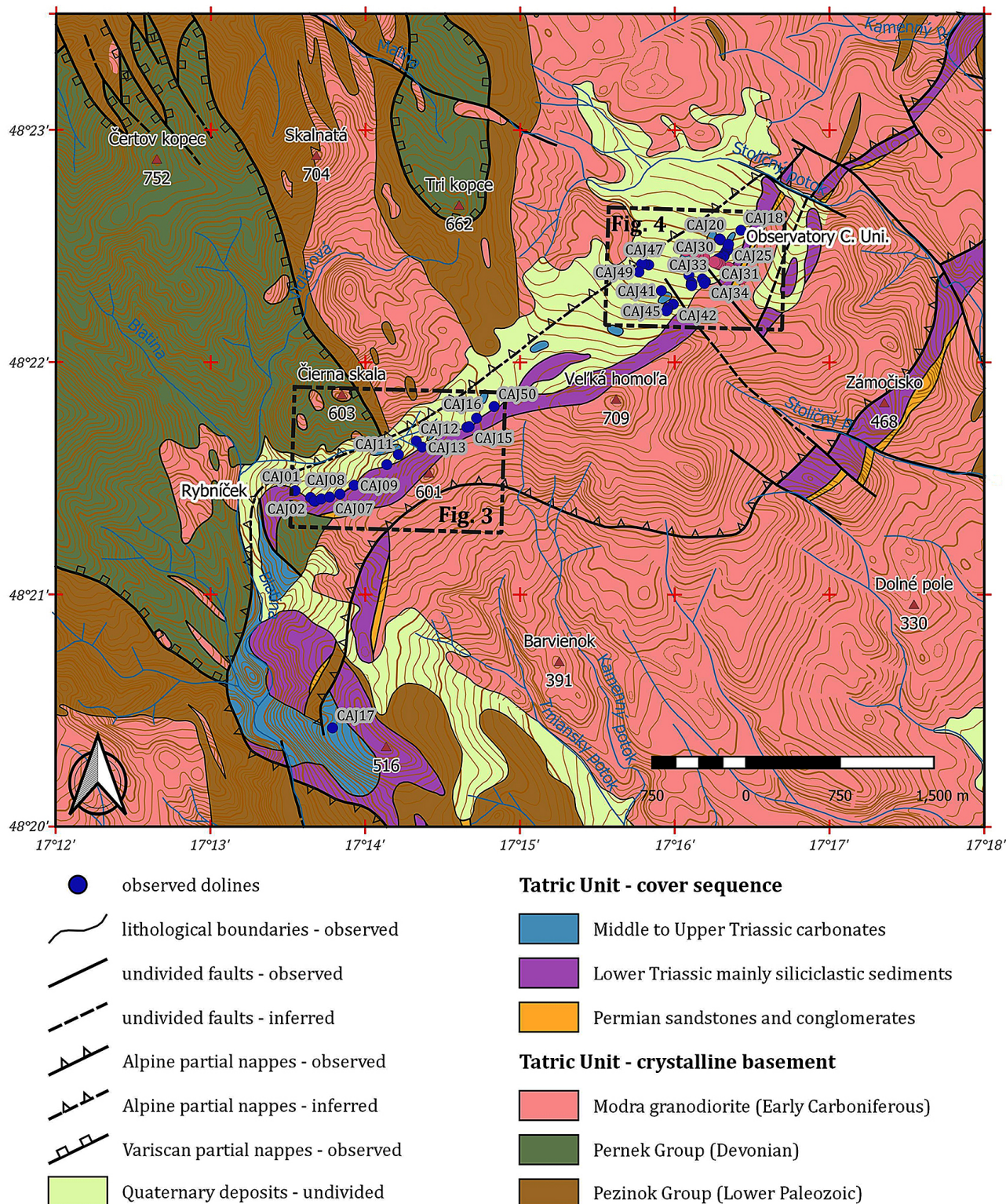


Fig. 2. Schematised tectonic map of the Malé Karpaty Mts. with the mapped dolines (according to Polák et al., 2011; modified).

sedimentary rocks (Pezinok and Pernek groups), which were intruded by the Modra granodiorite pluton (Koutek & Zoubek, 1936; Cambel, 1954; Méres, 2005).

The Tatric crystalline fundament is sealed by the cover sequence in autochthonous position on top of the basement. The sequence consists of Upper Permian-Mesozoic sedimentary deposits affected by low grade Alpine metamorphic overprint

(e.g., Plašienka et al., 1991). The sedimentary record starts with the Upper Permian to Lower Triassic quartzite and quartzitic sandstones, conglomerates, occasionally sandy shale of the Lúžna Formation. In some places, there are a few meters thick irregular sedimentary bodies of arkose sandstones of the Devin Formation in its substratum. The quartzite bedding is inclined from 30° to 50° northwestwards and it is outcropped at the main ridge

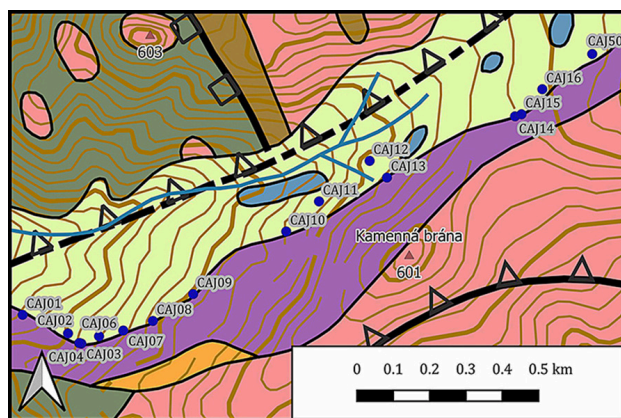


Fig. 3. Detailed schematised tectonic map of the Rybníček area with the mapped dolines (according to Polák et al., 2011; modified). For explanation, see Fig. 1.

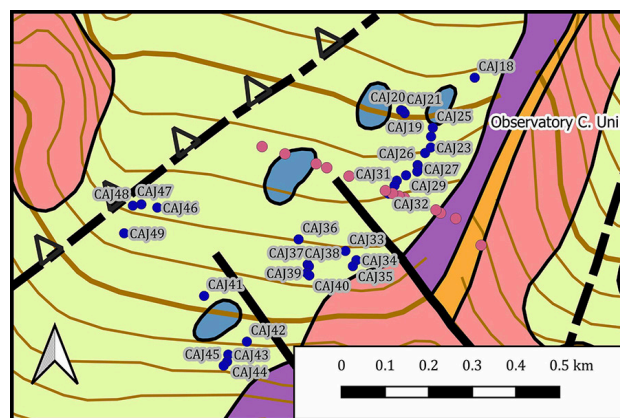


Fig. 4. Detailed schematised tectonic map of the area near Comenius University Observatory with the mapped dolines (according to Polák et al., 2011; modified). For explanation, see Fig. 1.

from the Tisové skaly through Veľká Homoľa hill (709 m a.s.l.) to Kamenná brána hill (601 m a.s.l.). Towards the overlying strata (to the NW), siliciclastic sediments pass to grey limestone and dolomite. This carbonate succession is estimated to be the Anisian to Ladinian in age, although no biostratigraphic data are available. Based on the position, they are considered to be the Gutenstein Formation with dolomitic carbonates and Ramsau Dolomite (Polák et al., 2011). Dolines were formed mainly in the Gutenstein Formation and at the contact of quartzite of the Lúžna Formation. Limestone and dolomite are grey in colour, layered to massive and are permeated by numerous systematic joints. In several places, they are influenced by pressure solutions and spaced to pressure solution cleavage is partly formed. Younger rocks than the Ladinian in age have not been preserved or they are unknown because the significant part of the carbonate rocks is covered by Quaternary slope debris, which consists predominantly of loamy-gravelous, sandy-gravelous to bouldery sediments from local materials.

The Cajla Karst is located within the tectonically duplexed Tatric crystalline basements with monoclinical structure and with the general dipping northwards. The sedimentary succession of the cover sequence is lying on top of the lower duplex of the crystalline basement located southeast of the karstic area and represents the Modra granodiorite partial nappe. From the other side, the cover succession is overridden by the upper duplex (Baďurka partial nappe) of the crystalline basement located in the northwestern part (e.g., Maheľ, 1986). The strike of the thrust plane of the upper duplex is oriented in the NE–SW direction with the northwestward inclination (Fig. 2). The imbricated structure was most probably formed during the Eo-Alpine (Cretaceous) tectonogenesis. However, early Miocene backthrusting tectonics cannot be excluded. Later, during the Cenozoic, this structure was significantly segmented by NW–SE striking faults. They represent a distinct geomorphological feature of the karstic area. Along the faults, distinctive valleys have been formed with surface watercourses following the structures subsequently.

The Cajla Karst has developed in this zone of the intricately folded Middle Triassic limestones and dolomites (mainly Gutenstein Formation) of the Tatric Unit on the N–NW rim

of Cajlanská Veľká Homoľa hill (516 m a.s.l.) (Mitter, 1983). A belt of karstic rocks expands from the locality of Rybníček at Veľká Homoľa hill (709 m a.s.l.) to the Tisové skaly, where the Astronomic observatory of the Comenius University is located. The karst is covered with Pleistocene to Holocene slope debris loamy-rocky, boulder to blocky and alluvial sediments with thickness of 30 m, which on some places exceeded 50 m (Bizubová et al., 2000). This belt continues to the settlement of Píla, at the spot height of Kukla hill (564 m a.s.l.). On the eastern slopes, the terrain is divided with deep valleys of hillside streams expanding from the ridge of the southern part of the Malé Karpaty Mts. belonging to the Modra granodiorite massif. The substratum for karstification consists of Gutenstein limestones and Ramsau dolomites (Anisian–Ladinian) of the Tatric cover sequence, whereas in the Modra surroundings Palaeozoic marbles and hornfels of the Pezinok Group can also be karstified (Polák et al., 2011). Underground karstic forms include the Cajla Cave (also called Tibra; length = 75 m), Malá jaskyňa v lome Cave (also called Tank; length = 7 m), the Pec Cave (also called Jaskyňa pri ceste Cave; length = 25 m) located close to the main road to Baba (536 m a.s.l.), and Braňov závrť Cave (length = 30 m) (Hochmuth, 2008).

Our research was focused on the part of the karst area with the karstic rocks extending in the belt from the gamekeeper's lodge Rybníček at the entrance to the Hrubá valley through Veľká Homoľa hill (709 m asl.) to the Tisové skaly (480 m asl.). Here, the Gutenstein Formation is overlain by loamy-gravelous, boulder, and block slope debris. The research goal was to explain the formation of dolines, which are localised in the belt in the NE–SW direction, extended in the length of 4 km. Apart from Šmída (2008), who briefly mentioned 38 depressions, the presence of dolines in the area of Piesok and Zochová chata at Modra-Harmónia was mentioned also by Bizubová et al. (2000). They classified the area as the cryptokarst, formed in slope debris deposits, with underlying limestones. They described depressions, similar to karstic holes, with the depth exceeding 5 m, but without exposed carbonates. Even when excavated the flat bottom of one of such holes into the depth of 1.6 m, carbonates were not identified there. Bizubová et al. (2000) also published a

topographic profile section of the slopes and the bottom of one of such depressions (these authors consider it to be “pseudokarst”), which were filled with loess (transformed to cambisol) overlying the quartzite and granite debris deposits. In the light of current understanding, these forms cannot be classified as cryptokarst but rather as the covered karst.

3. METHODS

For locating dolines, as well as for providing the historical context of speleological works in the dolines, a cooperation with a local speleologist group (Speleo Bratislava) was required. Several tools were used during the field research, including a GPS toolkit, laser rangefinder, inclinometer with compass (Leica Disto D3), measuring tape, geological compass, and a camera.

During the morphometric analysis, several previously published case studies were followed, which were focused on the karstic areas of the Malé Karpaty Mts. (e.g., Veselský et al., 2014^a, 2014^b, Lačný et al., 2019, 2020). Moreover, to the exact location of the dolines, we also documented in several directly measurable attributes: elevation, perimeter, depth, the longest axis, azimuth of the longest axis, and the inclination of the walls. The dolines were categorised in the field based on their shape in map view as round, oval or irregular.

The geographical coordinates of the dolines obtained from our fieldwork were transformed and recorded in a geographical information system (GIS). Visualizations were made using QGIS Desktop 3.18.0 “Zurich” and GRASS-GIS 7.8.5 (QGIS.org, 2020; GRASS Development Team, 2020). The final maps illustrate relevant parameters of dolines such as perimeter, depth and orientation of the longest axis, all pictured on hillshaded DTM (Digital Terrain Model), which was created from processed and classified LiDAR data using LASTool. The data were acquired within the National project for aerial laser scanning of the Slovak Republic (Leitmannová & Kalivoda, 2018).

Three surface geophysical methods were applied obtaining more detailed characterisation of shallow subsurface structure (down to the depth of few tenths of metres) of selected doline (CAJ32) to test the assumed geological model. Soil radon emanometry method (Rn) belongs to atmo-geochemical techniques and is based on measurement of alpha radiation originating in soil air samples taken from the depth of approx. 0.8 m and their immediate in situ analysis in scintillation radon detector. The method offers the curve of the ²²²Rn activity concentration (RAC) values (in kilobecquerels per cubic meter, kBq.m⁻³) in near-surface horizon along the studied profile. These measurements were intended to specify the fault position or the part of the geological environment most permeable for gases. The portable radon detector LUK 3R (SMM Prague, Czech Republic) was used for field measurements. 2D electrical resistivity tomography (ERT) line was collected using an ARES instrument (GF Instruments Inc., Czech Republic). The survey was 475 m long using a dipole-dipole array configuration with 5 m electrode spacing. In total 96 electrodes were used simultaneously. For post-processing and data interpretation, the inversion program RES2DINV (Loke & Barker, 1996) was applied. It generates a

topographically corrected 2D resistivity model of the subsurface by inverting the apparent resistivity data. Robust inversion (L1 norm) was used because it is more suitable for detecting sharp linear features such as faults. Seismic refraction tomography (SRT) uses controlled source seismic waves to determine the depth of seismic interfaces below the surface and velocity of propagation (vp) of seismic waves between designated interfaces (Lilie, 1999). Seismic waves propagate from the source and the arrival of each wave is detected along the geophone line. Refraction seismics uses direct waves and critically refracted waves that arise on individual interfaces (Raynolds, 1997). Seismic refraction tomography is an alternative to conventional refractive seismic interpretation methods (Sheehan et al., 2005) which used inverse techniques to reconstruct sub-surface velocities. The data for SRT at the Cajla Karst locality were acquired by a 24-channel DMT equipment with 10 Hz vertical geophones and a hammer as the source of seismic waves. The profile of total length 175 m was measured by two overlapping lines of 115 m in length and overlapped by 12 geophones. On each of the lines, the geophone spacing was 5 m and the position of the source was shifted every 10 m, with the first shot 7.5 m before the first geophone and the last shot 7.5 m after the last geophone. The measured data were processed in Reflexw Version 8.0 software (developed by Sandmeier, 2016) by processing methods for refractive seismics and seismic refraction tomography.

4. RESULTS

4.1. Field observations and morphometric analysis

In the study area 50 dolines were identified (Tab. 1), which are located at the contact of quartzite of the Lúžna Formation and Gutenstein limestone and dolomite (Figs. 3,4). Anthropogenic forms in Palaeozoic marbles and hornfels in the area of Modra-Harmónia and Zámčisko (470 m asl.) are herein considered as anthropogenically processed via mining (heaps and traces of mining activities).

Moreover, a large number of anthropogenically processed pits are also located here, used for limestone mining and its subsequent processing to lime. Physical measurement of dolines was very important, as it was needed to distinguish anthropogenically processed holes from studied dolines. The largest number of anthropogenically processed pits are located in the vicinity of Vápenka (590 m asl.), where the carbonate is exposed on the surface. Mining pits can be distinguished from dolines by the presence of remains from burning lime (ash, remains from sintering, small slag heaps). According to historical maps, several quarries were located there. During our research, we have found several pits without remnants from burning lime. We suggest that these were test pits for evaluation of limestone for further processing.

Altogether, 49 dolines are arranged in the line (besides CAJ-17, Braňov závr Cave) (Figs. 5–8). They originated on the contact of quartzite of the Lúžna Formation and overlying carbonate of the Gutenstein Formation. Generally, the dolines are located on slightly inclined platform, with the inclination of 1–5°. However,

Tab. 1: An overview of depressions with relevant parameters and coordinates in the System of the Unified Trigonometrical Cadastral Network (S-JTSK, EPSG: 5514)

Doline Designation	x (S-JTSK)	y (S-JTSK)	Altitude [m asl.]	Perimeter [m]	Depth [m]	Longest Axis [m]	Azimuth of Longest Axis [in degrees]	Inclination [in degrees]	Category
CAJ-01	562634.365	1258095.960	406	74	3	21,14	263	20	irregular shape
CAJ-02	562521.225	1258165.540	464	57	2	15	302	16	irregular shape
CAJ-03	562484.896	1258203.460	469	42	4	12.32	146	25	irregular shape
CAJ-04	562491.845	1258186.540	467	65	5	17.46	69	26	irregular shape
CAJ-05	562476.165	1258189.390	466	43	1.7	11.98	86	12	irregular shape
CAJ-06	562439.826	1258183.360	472	48	2	14.4	99	20	irregular shape
CAJ-07	562362.178	1258180.270	470	120	8	31	110	37	irregular shape
CAJ-08	562277.773	1258162.490	490	69	1.5	15.96	310	19	oval shape
CAJ-09	562148.258	1258098.650	501	79	3.5	22.4	58	23	irregular shape
CAJ-10	561881.608	1257958.620	526	92	4.5	24.88	50.3	32	oval shape
CAJ-11	561781.763	1257887.920	528	77	2	14.68	112	28	oval shape
CAJ-12	561627.259	1257794.260	552	30	1.2	7.8	137	14	oval shape
CAJ-13	561589.673	1257855.270	560	38	1	12.24	76	10	oval shape
CAJ-14	561219.416	1257727.660	587	81	4	18.3	350	35	irregular shape
CAJ-15	561201.054	1257724.240	587	85	3	22.09	68	27	oval shape
CAJ-16	561135.328	1257663.170	593	45	3.5	17.74	12	32	oval shape
CAJ-17. Braňov závrť	562523.194	1260009.000	468	95	4	23.68	54	37	irregular shape
CAJ-18	558887.227	1256379.240	484	27	1.5	8.84	306	27	irregular shape
CAJ-19	559057.149	1256439.710	495	38	2	11.56	313	17	oval shape
CAJ-20	559064.375	1256431.510	495	44	1.2	16.32	27	14	irregular shape
CAJ-21	559060.906	1256433.300	492	66	1.7	25	231	18	irregular shape
CAJ-22	559022.270	1256536.140	500	100	6	31	40	36	oval shape
CAJ-23	559007.561	1256525.190	500	55	1.8	19.48	42	22	oval shape
CAJ-24	559003.839	1256500.420	496	54	2	16.1	257	23	irregular shape
CAJ-25	558997.271	1256480.730	495	65	1.8	10.4	75	19	oval shape
CAJ-26	559045.066	1256568.720	505	59	1.7	20.9	250	29	irregular shape
CAJ-27	559050.843	1256590.110	510	25	1.5	8.25	79	29	oval shape
CAJ-28	559058.910	1256593.520	511	27	1.7	7.76	67	39	oval shape
CAJ-29	559072.231	1256581.240	504	133	5	49	38	29	irregular shape
CAJ-30	559094.762	1256590.740	510	95	4	26.4	27	24	irregular shape
CAJ-31	559101.389	1256601.260	510	103	6	33	117	30	irregular shape
CAJ-32	559117.469	1256617.760	512	87	3.5	26	178	27	irregular shape
CAJ-33	559232.497	1256735.630	533	18	1	4.9	226	22	oval shape
CAJ-34	559209.673	1256764.000	535	40	1	12.4	219	15	oval shape
CAJ-35	559225.382	1256774.280	536	23	0.5	7.2	212	14	oval shape
CAJ-36	559333.683	1256698.370	531	23	1.2	6.36	198	23	oval shape
CAJ-37	559327.298	1256757.190	535	66	4	21	49	22	irregular shape
CAJ-38	559312.723	1256762.840	537	79	4.5	23	149	27	irregular shape
CAJ-39	559326.740	1256774.560	538	40	1.5	11.4	191	19	irregular shape
CAJ-40	559321.258	1256781.350	539	48	2.5	16.9	231	25	irregular shape
CAJ-41	559568.810	1256803.390	546	33	2	9	128	30	oval shape
CAJ-42	559483.361	1256913.100	557	50	3	15.2	104	22	oval shape
CAJ-43	559529.597	1256937.120	563	44	1.5	11.8	179	18	irregular shape
CAJ-44	559536.991	1256951.250	565	19	1.5	5	40	32	oval shape
CAJ-45	559550.367	1256959.850	567	17	1	5.8	132	19	oval shape
CAJ-46	559647.811	1256581.550	529	40	1	12.4	90	13	irregular shape
CAJ-47	559690.262	1256573.170	531	58	1.3	16.1	19	15	oval shape
CAJ-48	559708.652	1256577.940	532	36	2.5	12	72	23	irregular shape
CAJ-49	559728.915	1256641.630	540	21	0.8	6.5	326	30	irregular shape
CAJ-50	560995.858	1257578.390	595	37	1	12.48	274	15	irregular shape

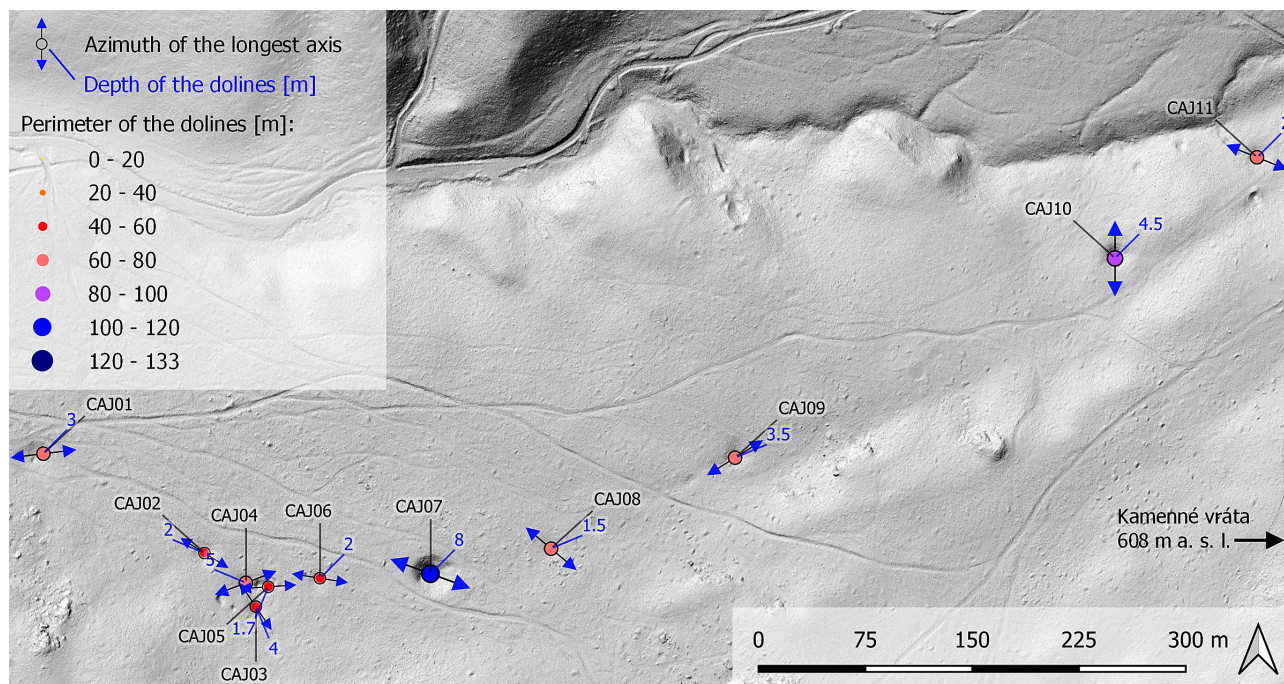


Fig. 5. Location of dolines on Rybníček site.

some dolines were formed on higher slope platforms. The immediate infiltration of water into underground structures from the quartzite is the reason of doline formations. Close to the contact of quartzite and limestone, funnel-shaped dolines are dominant, sometimes with half-open to open bottoms. Further

from the main line, cup-shaped dolines with flat, sometimes muddy, bottoms are dominant. In 11 dolines inflow lines were identified, or their bottoms had active submersions, which infiltrated the water into the underground during heavy raining or snow melting (CAJ-01, 07, 09, 15, 18, 26, 29, 32, 38, 40, 41).

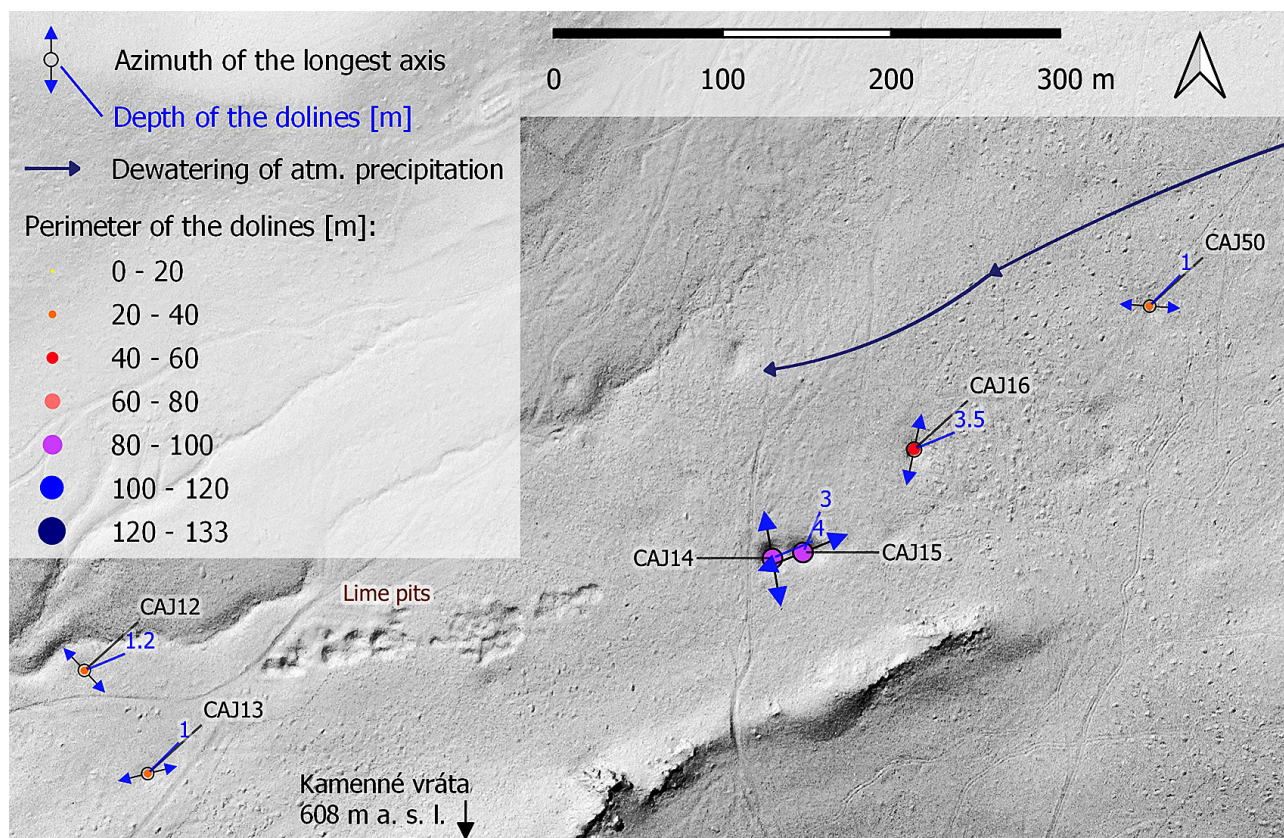


Fig. 6. Location of dolines on Kamenné vrata site.

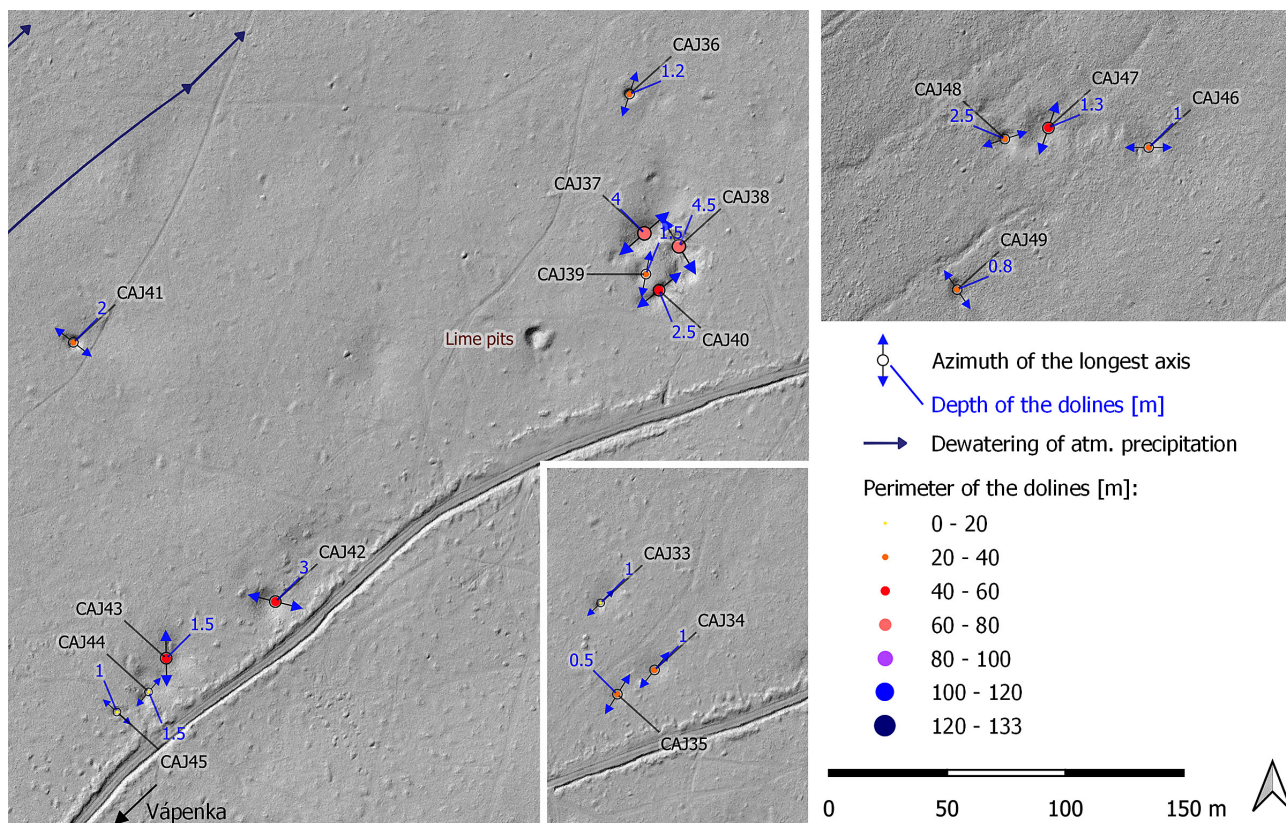


Fig. 7. Location of dolines on Homola site.

The size of dolines is heterogeneous (Figs. 5–8). In the area, uvalas are also present. Mostly, two or more dolines are interconnected. The highest number of such dolines are located close to the road to the observatory (CAJ-22 – CAJ-32) (Fig. 8); between the respective dolines the boundaries were removed at several places. Some dolines can be identified as mother and daughter dolines, sometimes called also parasitic dolines or depressions. Based on their top view, irregular dolines (28) dominate over oval ones (22) (Tab. 1). Irregularity was caused by dynamic conditions resulting in formation of inflow lines and interconnected dolines via removing boundaries. Based on the doline size, the area is relatively heterogeneous. There are dolines with the perimeter over 100 m (CAJ-22, 31, 07, 29). As many as 25 dolines have a perimeter of 10–50 m and this makes them typical dolines for the Malé Karpaty Mts. region. Their distribution is shown in Fig. 9A. The largest, previously described dolines are 5–8 m deep (Fig. 9B). The most frequently represented group of dolines include the forms with the depth of 1.1–2 m (22 dolines), followed with dolines with the depth of 0–1 m (8 dolines), and 3.1–4 m (8 dolines) (Fig. 9B).

Documented longest doline axes are more variable, when compared to data collected previously (Fig. 9C). Dolines with the longest axis of 4–17 m are most numerous (Fig. 9C). Studied dolines are located at the heights of 406–595 m asl. As far as the height above the sea level concerns, the highest were CAJ-50 (595 m asl.) and CAJ-14–16 (587–593 m asl.). Concerning the water drainage, the elevation north of Veľká Homola hill divides the line of dolines into two groups. The highest spot in the line of dolines is 629 m asl. From this spot, the water is drained into two

directions, i.e. southwest into the area of Rybníček (Figs. 5, 6) and northeast into the area of Tisové skaly (Figs. 7, 8). Furrows originated from surface water streams follow the same pattern. Azimuths of the longest axes were plotted in a rose and contour diagrams and indicate two main directions, i.e. NE–SW and NW–SE (Fig. 10).

4.2. Geophysical research

The aim of the geophysical research was to explain the genesis of distinct depressions occurring in the close vicinity of the Tisové skaly. Since some of them were probably anthropogenically affected, it was not possible to demonstrate whether these were natural forms or mining pits. Difficulty in determination of the possible anthropogenic origin was caused also by absence of carbonates in the surroundings, which were covered with slope debris sediments.

The quartzite bedding near the geophysical profile (Fig. 8) is inclined from 30° to 45° northwestwards. Also, the subvertical fissures directed to northwestwards, were measured, which probably related to fault structures of these directions.

Geophysical methods were applied along the NW–SE profile crossing the CAJ32 doline (Fig. 8). The ERT measurements cover the longest part of 475 metres while the seismic and radon emanometry ones cover about 100 (radon emanometry) and 175 (seismic methods) metres-long part with the CAJ32 doline in the centre (Fig. 11).

As follows from the course of the ^{222}Rn activity concentration (RAC) in soil air (Fig. 12) the geophysical differentiation

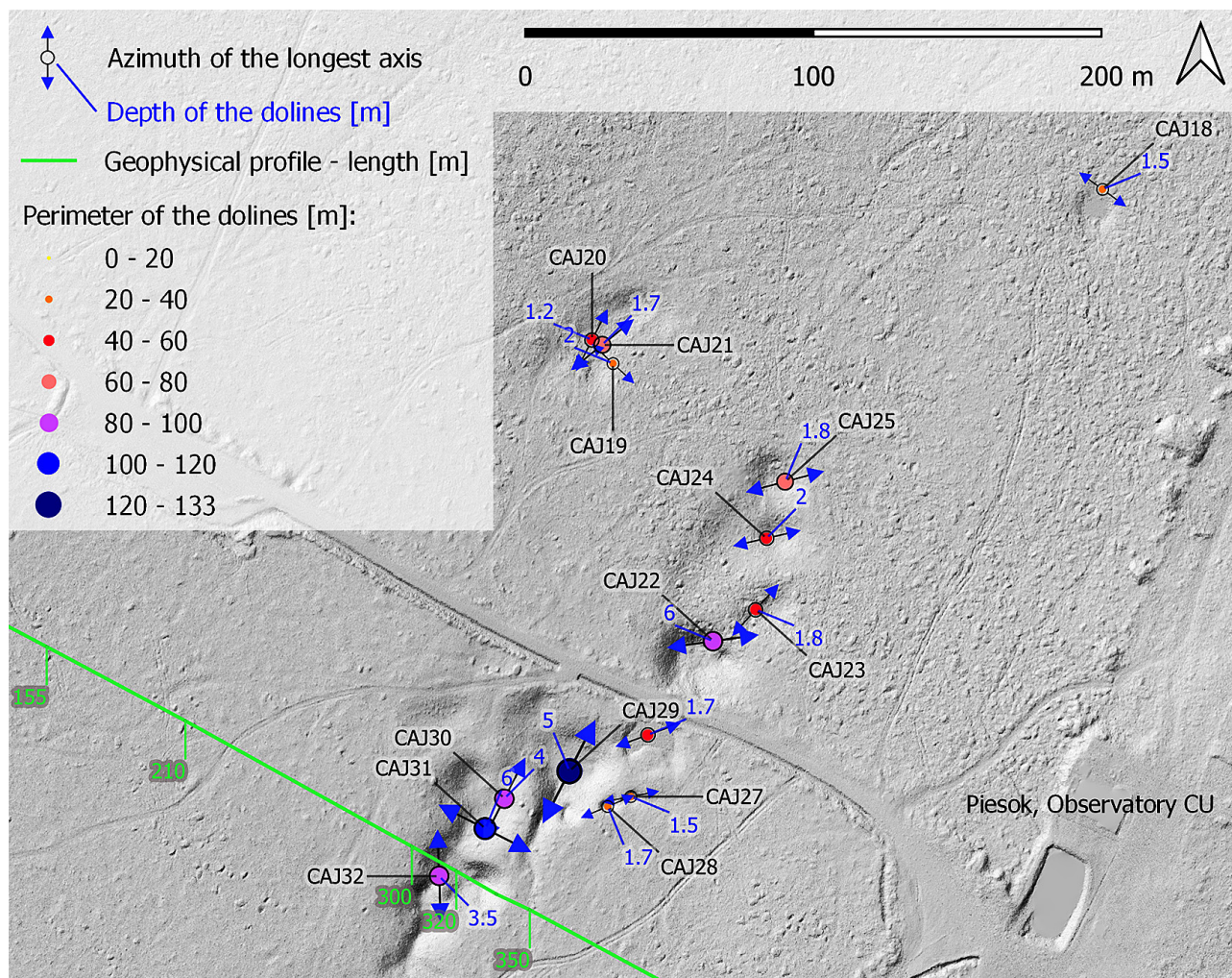


Fig. 8. Location of dolines on Comenius University Observatory site.

between parts of slope debris sediments of different petrophysical properties could be claimed to certain extent. Based on an average lower values of RAC (around $18 \text{ kBq}\cdot\text{m}^{-3}$) at the SE end of profile, starting from station of 120 m, this geological environment represents the less bouldery and less permeable part that is waterlogged at the stations of 135, 140 and partly also 150 m (possible relation to weathered quartzite). The part with an average higher values of RAC (around $37 \text{ kBq}\cdot\text{m}^{-3}$) at the NW half of profile up to the station of 120 m, could be attributed to the more bouldery and more permeable one (possible relation to weathered limestone). The highest values of RAC up to $70 \text{ kBq}\cdot\text{m}^{-3}$ localised at NW slope foot of CAJ32 doline (stations 90–100 m) and at station of 70 m could indicate the presence of deeper tectonics and could be an evidence of tectonic origin of the doline.

The result of SRT data processing is a velocity profile (Fig. 13A). There is a subvertical contact of slope debris deposits ($v_p < 1500 \text{ m}\cdot\text{s}^{-1}$) with quartzite ($v_p > 3000 \text{ m}\cdot\text{s}^{-1}$) in the SE part of this SRT velocity profile. This interface corresponds with the interface interpreted at the ERT profile. The other deeper contacts and tectonic faults are not captured at the SRT velocity profile because of survey depth range which is given by maximum offset of survey.

In the ERT cross section (Fig. 13B), the resistivity values range between $80 \Omega\cdot\text{m}$ and about $2500 \Omega\cdot\text{m}$ and a significant vertical contrast between two blocks can be seen at the same position as in the seismic section. The most significant is contact between the quartzites and weathered limestones and dolomites.

The quartzites block is characteristic for his highest resistivity values ($> 1900 \Omega\cdot\text{m}$), while in the limestones and dolomites block, the resistivity values are smaller (from $700 \Omega\cdot\text{m}$ to $1200 \Omega\cdot\text{m}$). The resistivity contrast between the quartzites and weathered limestones is detected at approximately 340 m from the beginning of the profile (Fig. 13B). The layer of slope debris sediment covers the quartzites, limestones, and dolomites. The resistivity of this layer is from $80 \Omega\cdot\text{m}$ to $600 \Omega\cdot\text{m}$, which reaches a thickness of up to 50 m. This geological section was constructed from the results of geophysical measurements (Fig. 13A,B).

5. INTERPRETATION AND DISCUSSION

The karst in the study area with the occurrence of a line of dolines is covered by slope debris deposits. Based on visual observation in the field, these are up to several tens of metres thick and contain small debris but also occasional larger blocks of quartzites, which

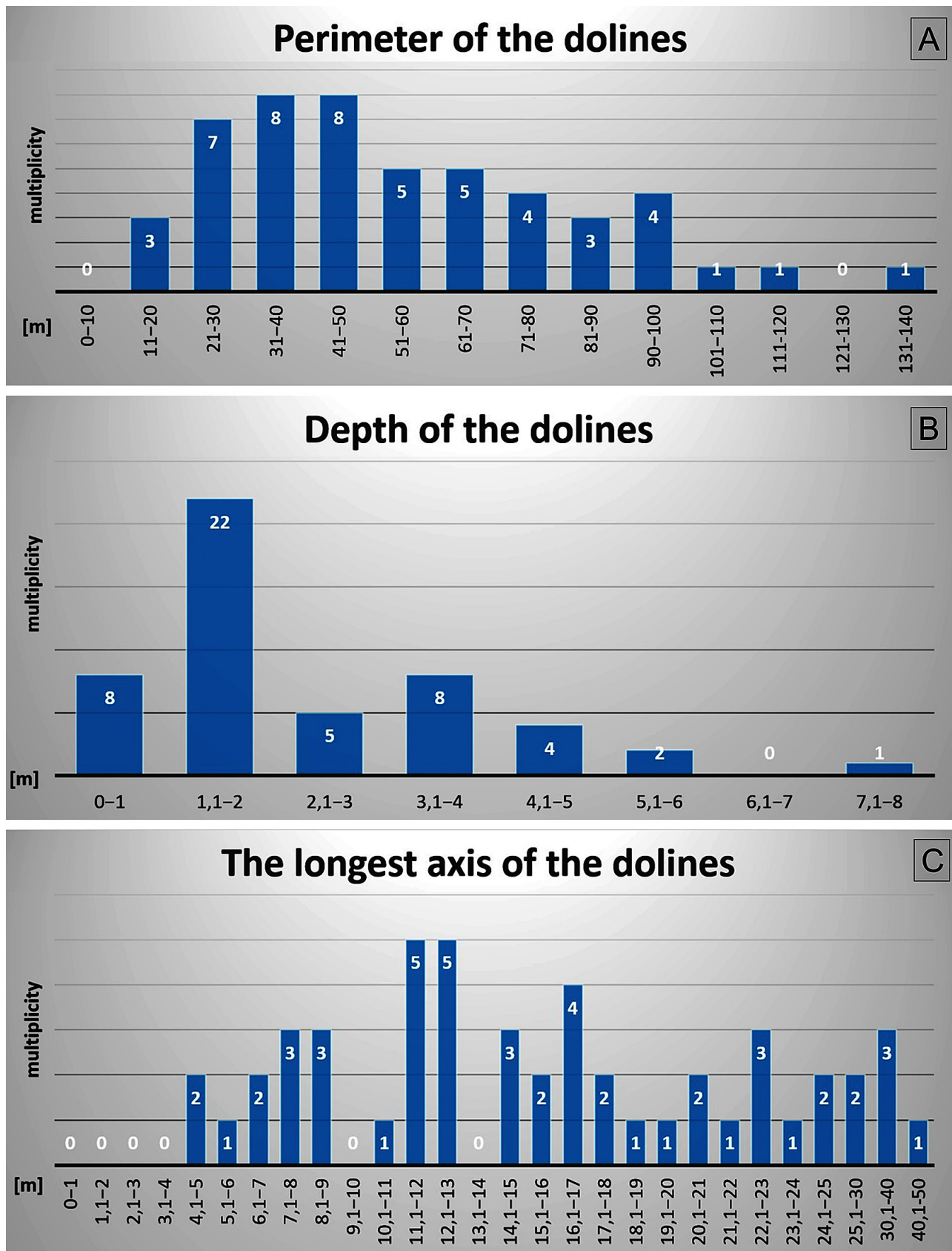


Fig. 9. A – Graph showing multiplicity of dolines based on their perimeter; B – Graph showing multiplicity of dolines based on their depth; C – Graph showing multiplicity of dolines based on their longest axis.

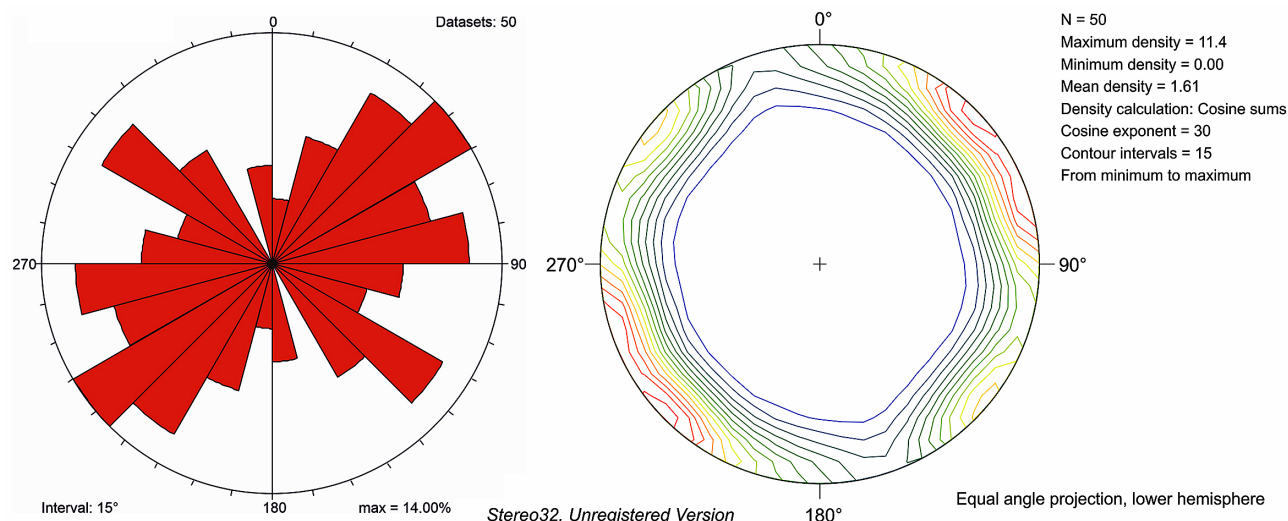


Fig. 10. Rose and contour diagrams of measured 50 azimuths of the longest doline axes.

were transported here from a nearby ridge of Velká Homoľa hill (709 m asl.). In the slope deposits, Gutenstein carbonate are present as well, usually as occasional debris, although larger blocks with the diameter of several metres were also observed. In other areas, carbonate is exposed on the surface as small “islands” isolated in slope debris and alluvia deposits. They are markedly exposed in the surrounding of the spot height Vápenka (590 m asl.), located north of Velká Homoľa hill (709 m asl.) (Fig. 3).

Genetically, most of the dolines of the Cajla Karst can be considered as a result of the corrosive effects of surface precipitation, concentrated into inflow lines and they are dominated over collapsed weakened ceilings of the caves. As far as the genesis concerns, funnel-shaped dolines can be considered as accelerated solution dolines (*sensu* Sauro, 2003). These can be further subdivided into two common types, including point recharge dolines and “common” accelerated corrosion dolines (draw-down dolines). A difference between these types is in the water draining; in the “common” accelerated corrosion doline type a vertical draining dominates, whereas in the second type inclined draining from a single direction dominates.

Eleven dolines can be defined as a point recharge doline type. Other funnel-shaped doline forms close to the contact of the karst and non-karst can be characterised as “common” accelerated corrosion doline type (drawdown doline) (e.g., CAJ-14, 22, 28, 44, 49). In shallower cup-shaped forms, further from the main line, underground dissolution/dissolvement may dominate. These dolines can be considered as subsidence dolines (*sensu* Sauro, 2003).

Inflow lines, sometimes inverted bottoms, indicate a corrosion dolines. In CAJ17, not far from the line, there is a doline with inflow line. Speleologists discovered the corrosive Braňov závrť Cave (length = 30 m) in this place. The situation is different in the area of the Observatory CU, where there is a thicker layer of slope debris sediments, where shallow forms of subsidence dolines dominate further from the line.

A geological section was constructed from the results of geophysical measurements (Fig. 13A,B). The geological interpretation of the geophysical section is shown in Fig. 13C. We assume

that the weathered carbonates are located in the vertical distance from about 20 m to 60 m in the form of normal faults. Therefore, the thickness of slope debris deposits is not the same. The doline CAJ 32 was formed under a relatively thin layer of slope debris deposits about 15–20 m. The reason for this is also the close contact of quartzites protruding to the surface.

Azimuths of the longest axes of dolines indicate two main directions, i.e. NE–SW and NW–SE (Fig. 10). The NW–SE direction follows the main doline line, which is the tectonised line of lithological boundary between quartzites and carbonates. Maximal elongation of the axes of the studied dolines in this direction could be caused by surface water outflow and subsequent infiltration from the highest spot (629 m asl.) in the direction to NE into the area of Tisové skaly and to SW into the area of Rybníček. Also, more inflow lines follow this direction.

The NW–SW direction of the maximal elongation of the doline axes influenced the water inflow to the underground from the main ridge of Velká homoľa hill (709 m a.s.l.), which is built of quartzites and which is located SE from the line of dolines. In the contact with carbonates, a distinctive infiltration and



Fig.11. Geophysical profile realised above study depression CAJ32. Photo: A. Lačný

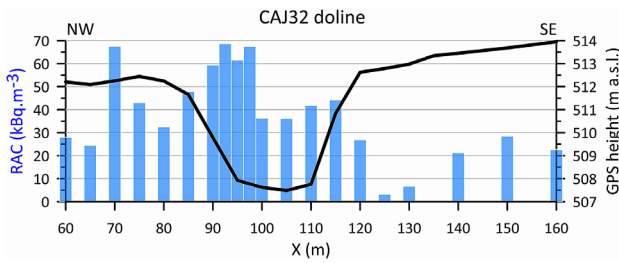


Fig. 12. Graphs of ²²²Rn activity concentration (RAC) in soil air and topography along geophysical profile crossing the CAJ32 doline (X-scale identical to the seismic refraction section in Fig.13)

boundaries and that subhorizontal topography is not essential for the doline formation. If the contact infiltration zone is at a steeper angle, a doline was formed as well. Based on the location and size of the dolines, the Cajla Karst can be determined in terms of geomorphic evolution of karst as a young type karst (*sensu* Grund, 1914).

The implementation of geophysical measurements confirms the importance of interface of quartzite and limestone, which are covered by a relatively thick layer of Quaternary slope and alluvial deposits. The contact between the subsoil and the Quaternary sediments was captured by both ERT and SRT measurements. The ERT section detected also the tectonic contact of

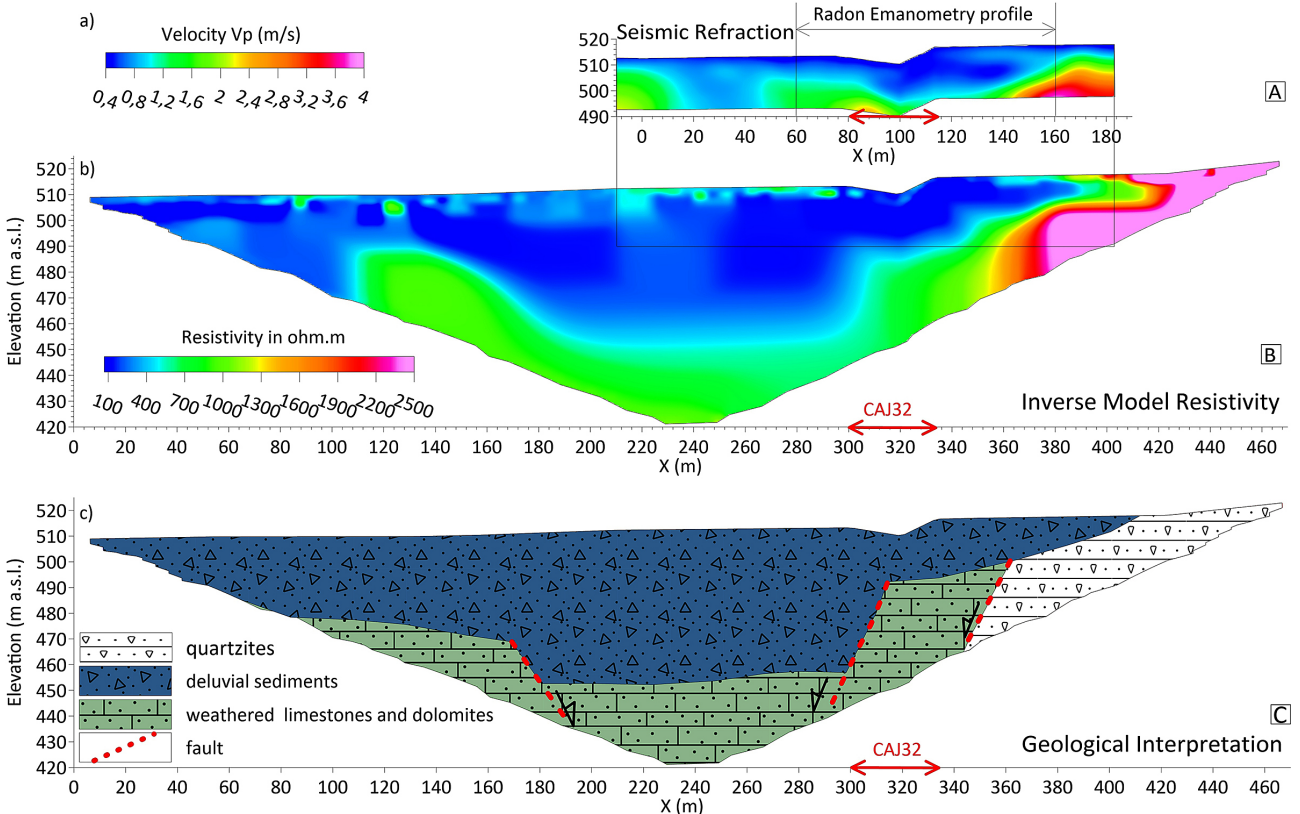


Fig. 13. Display the results of the resistivity inversion and seismic refraction tomography along the profile.

morphology of dolines in this direction can be observed. Such orientation can be caused also by brittle fault structures of such affinity occurring in the area (Figs. 3, 4).

6. CONCLUSION

In Slovakia a complex research of depressions originated in the covered karst comparable to the present study was not performed before. Dynamic conditions of the contact zone of the karsts and non-karst, surface water outflow and subsequent infiltration of water into underground were the factors with major influence on the irregular shape/top view of studied dolines. The dynamics of the environment was further enhanced by as many as 11 inflow lines and several active submersions on doline bottoms. The specificity of the karst is origin on the significant lithological

carbonate and quartzite in the subsoil of Quaternary sediments. The geological-geophysical section (Fig. 13) based on results of seismic and geoelectric measurements at the CAJ32 doline case, confirms an assumption of its formation due to the presence of NE–SW striking faults zone in underlying limestones and dolomites dipping to the NW. The fault is covered by a layer (a horizon) an accumulation of slope sediments first tenths of meters in thickness. This knowledge is also confirmed by the highest values of soil radon concentration (Fig. 12), rising upwards from the basement through fault zone and permeable Quaternary debris and alluvial cover, and their localisation at NW slope foot of the doline and also at NW direction from the doline (station 70 m).

The atypical location of some depressions initially evoked anthropogenic activity, making the area also specific. However, their natural character was confirmed by the appropriate use of

geophysical methods. The processes of formation of this specific karst were explained, which can also be applied to similar karst areas.

Acknowledgement: The geological and geomorphological research was carried out within the framework of the scientific grant project APVV-16-0146, and the Plan of main tasks of the State Nature Conservation of the Slovak Republic for 2020. Special thanks to our colleagues Michaela Galová and Richard Zipser from the Little Carpathians Protected Landscape Area for help with the field research. We thank the editor Michal Šujan and reviewers Márton Veress and Ludovít Gaál for their valuable advice and comments.

References

- Bizubová M., Kolény M. & Nováková M., 2000: Príspevok k poznaniu niektorých krasových území v Pezinských Karpatoch [Contribution to the knowledge of some karst areas in the Pezinské Karpaty Mts.]. *Slovenský kras*, 38, 155–163. [in Slovak with English abstract]
- Bondesan A., Meneghel M. & Sauro U., 1992: Morphometric analysis of dolines. *International Journal of Speleology*, 21 (1–4), 1–55.
- Cambel B., 1954: Geologicko-petrografické problémy severovýchodnej časti kryštalinika Malých Karpát [Geological-petrographic problems of the northeastern part of the crystalline basement of the Malé Karpaty Mts.]. *Geol. Práce, Zosít*, 36, 3–74. [in Slovak]
- Castiglioni B., 1991: Some morphometric and environmental aspects of dolines in Berici Hills (Vincenza, Italy). Proceeding of the International Conference on Environmental Changes in Karst. Areas-IGU-UIS, Quaderni del Dipartimento di Geografia nr. 13, Università di Padova, 143–155.
- Cvijijć J., 1893: Der Karstphänomen. *Geographische Abhandlungen*, 5, 219–329.
- GRASS Development Team, 2020: Geographic Resources Analysis Support System (GRASS) Software, Version 7.8. Open Source Geospatial Foundation; <https://grass.osgeo.org>
- Grund A., 1914: Die Geographische Zyklus im Karst. *Gesellschaft für Erdkunde*, 52, 621–640.
- Gvozdetkiy N.A., 1965: Types of Karst in the U. S. S. R. Separatum, Prob. Speleol. Res., Prague, 47–54.
- Hevesi A., 1986: Hideg vizek létrehozta karsztok osztályozása [Classification of Cold-Water Karsts]. *Földrajzi Értesítő*, 231–254. [in Hungarian]
- Hochmuth Z., 2008: Krasové územia a jaskyne Slovenska [Karst areas and caves in Slovakia]. *Geographia Cassoviensis*, 2, 2, 210 p. [in Slovak]
- Jakál J., 1975: Kras Silickej planiny. [Karst land of Silica Plain] Osveta, Martin, 149p. [in Slovak]
- Jakál J. & Bella P., 2008: Caves of the World Heritage in Slovakia. Správa slovenských jaskýň, Liptovský Mikuláš, 168 p.
- Koutek J. & Zoubek V., 1936: List Bratislava 4758. Vysvětlivky ke geol. mapě v M 1:75 000 [Explanations to the geological map at a scale of 1:75 000]. *Knih. St. geol. Úst. Čs. Republ.*, 18, 150 p. [in Czech]
- Kruse S.E., Grasmueck M., Weiss M. & Viggiano D., 2006: Sinkhole Structure Imaging in Covered Karst Terrain. *Geophysical Research Letters*, 33, 1–6.
- Lačný A., Kubičina L. & Csibri T., 2019: Morfometrická analýza závrvtov Čachtickej planiny [Morphometric analysis of sinkholes on the Čachtická Plain]. *Slovenský kras*, 57, 2, 147–164. [in Slovak with English abstract]
- Lačný A., Vojtko R., Veľšmid M., Dušková L. & Papčo J., 2020: Geological control of the origin of dolines in the Plavecký Karst (Malé Karpaty Mts., Slovakia). *Acta Geologica Slovaca*, 12, 2, 137–152.
- Leitmanová K. & Kalivoda M., 2018: Projekt leteckého laserového skenovania Slovenskej republiky [Aerial Laser Scanning Project of the Slovak Republic]. *Geodetický a kartografický obzor*, 64/106, 101–104. [in Slovak with English abstract]
- Loke M.H. & Barker R.D., 1996: Rapid least-squares inversion of apparent resistivity pseudosections by a quasi-Newton method. *Geophysical Prospecting*, 44, 131–152.
- Mahel M., 1986: Geologická stavba československých Karpát – Palealpínske jednotky 1. [Geological structure of the Czechoslovak Carpathians - Palealpine units 1]. Veda, Bratislava, 503 p. [in Slovak]
- Mazúr E. & Lukniš M., 1978: Regionálne geomorfologické členenie SSR [Regional geomorphological division of the SSR]. *Geografický časopis*, 30, 2, 101–125 [in Slovak]
- Méres Š., 2005: Major, trace element and REE geochemistry of metamorphosed sedimentary rocks from the Malé Karpaty Mts. (Western Carpathians, Slovak Republic): Implications for sedimentary and metamorphic processes. *Slovak Geological Magazine*, 11, 2–3, 107–122.
- Mitter P., 1983: Geomorfologická rajonizácia krasu Malých Karpát [Geomorphological regional division of the Malé Karpaty Karst]. *Slovenský kras*, 21, 3–34. [in Slovak with Russian abstract and English summary]
- Plašienka D., Michalík J., Gross P. & Putiš M., 1991: Paleotectonic evolution of the Malé Karpaty Mts. – an overview. *Geologica Carpathica*, 42, 195–208.
- Polák M., Plašienka D., Kohút M., Putiš M., Bezák V., Filo I., Olšovský M., Havrila M., Buček S., Maglay J., Elečko M., Fordinál K., Nagy A., Hraško L., Németh Z., Ivanička J. & Broska I., 2011: Geologická mapa Malých Karpát 1:50 000 [Geological map of the Malé Karpaty Mts. in scale 1:50 000]. State Geological Institute of Dionýz Štúr, Bratislava.
- Quinlan J.F., 1978: Types of Karst, with Emphasis on Cover Beds in Their Classification and Development. Dissertation thesis, University of Texas, Austin, 443 p.
- QGIS.org, 2020: QGIS Geographic Information System. Open Source Geospatial Foundation Project. <http://qgis.org>
- Sandmeier K.J., 2016: Reflexw – GPR and seismic processing software. Sandmeier geophysical research 2017 [cit. 2018-01-04]. Available on:<http://www.sandmeier-geo.de/reflexw.html>
- Sauro U., 2003: Dolines and sinkholes: Aspects of evolution and problems of classification. *Acta Carsologica*, 32, 2, 4, 41–52.
- Sauro U., 2012: Closed depressions in karst area. The Encyclopedia of Caves, 140–155.
- Segre A.G., 1948: I fenomeni carsici e la speleologia del Lazio. *Pubblicazioni dell'Istituto di Geografia dell'Università di Roma*, 7, 236 p.
- Sheehan J.R., Doll W.E. & Mandell W.A., 2005: An evaluation of methods and available software for seismic refraction tomography analysis. *Journal of Environmental and Engineering*, 10, 1, 21–34.
- Šmída B., 2008: Krasové jamy (závrty) Západných Karpát: štúdium ich morfológie a genézy [Dolines of the Western Carpathians: the study of the morphology and genesis]. Minimum thesis, Faculty of Natural Sciences, Comenius University in Bratislava, 113 p. [in Slovak]
- Trájer A.J., Mlinárik L., Hammer T., Földényi R., Somlai J. & Bede-Fazekas Á., 2020: Investigation of the vulnerability of a partly covered karst feature in Veszprém, Hungary. *Environmental Science and Pollution Research*, 27, 20410–20426.
- Upchurch S.B., Dobecki T.L., Scott T.M., Meiggs S.H., Fratesi S.E. & Alfieri M.C., 2013: Development of Sinkholes in a Thickly Covered Karst Terrane. 13th Sinkhole Conference, National Cave and Karst Research Institute Symposium 2, 273–278.

- Veress M., 2016: Classification of Covered Karsts. Covered Karsts, Springer Geology, Chapter 4, 97–205.
- Veress M., 2020: Karst types and their kartification. *Journal of Earth Science*, 31, 3, 621–634.
- Veselský M., Lačný A. & Hók J., 2014^a: Závrtý na Dlhom vrchu: modelová štúdia ich vzniku na lineárnych diskontinuitách (Malé Karpaty) [Dolines on Dlhý vrch hill: case study of doline evolution on linear discontinuity (Malé Karpaty Mts.)]. *Acta Geologica Slovaca*, 6, 2, 59–168. [in Slovak with English abstract and summary]
- Veselský M., Ágh L., Lačný A. & Stankoviánsky M., 2014^b: Závrtý na krasovej plošine Biela skala a ich morfometrická analýza, Kuchynsko-orešanský kras, Malé Karpaty [Sinkholes on the karst land of Biela skala and morphometric analyses, Kuchyňa-Orešany Karst, Malé Karpaty Mts.]. *Slovenský kras*, 52, 2, 127–139. [in Slovak with English abstract and summary]
- Waltham T., Bell F. & Culshaw M., 2005: Sinkholes and subsidence. Karst and Cavernous Rocks in Engineering and Construction, 1–225.
- White W.B., 1988: Geomorphology and Hydrology of Karst Terrains. Oxford University Press, New York, Oxford, 464 p.
- Williams P.W., 1972: Morphometric analysis of polygonal karst in New Guinea. *Geological Society of America Bulletin*, 83, 3, 761–796.
- Williams P., 2004: Dolines. In: Gunn J. (Ed.): *Encyclopedia of Caves and Karst Science*. Taylor and Francis Group, London, 304–310.